ISSN 1070-3632, Russian Journal of General Chemistry, 2014, Vol. 84, No. 1, pp. 33–39. © Pleiades Publishing, Ltd., 2014.
Original Russian Text © N.A. Magdalinova, P.A. Kalmykov, M.V. Klyuev, 2014, published in Zhurnal Obshchei Khimii, 2014, Vol. 84, No. 1, pp. 35–42.

Hydrogenation Catalysts Based on Platinum- and Palladium-Containing Nanodiamonds

N. A. Magdalinova, P. A. Kalmykov, and M. V. Klyuev

Ivanovo State University, ul. Ermaka 39, Ivanovo, 153025 Russia
e-mail: mn2408@mail.ru, klyuev@inbox.ru

Received January 14, 2013

Abstract—Platinum and palladium nanoparticles of 4–5 nm size applied at nanodiamonds have been shown to efficiently catalyze liquid-phase hydrogenation of different organic compounds (nitrocompounds, azomethines, and unsaturated hydrocarbons and alcohols) under mild conditions (T = 318 K, hydrogen pressure of 0.1 MPa, solution in ethanol). Using of palladium on nanodiamond containing 3 wt % of metal has been most efficient.

DOI: 10.1134/S1070363214010083

Platinum- and palladium-containing catalysts are widely used in various chemical and petrochemical processes. Activated carbons containing platinum or palladium are commercially available. Recently, carbon nanomaterials such as fullerenes and fullerene black [1, 2], carbon nanotubes and nanofibers [1, 3, 4], nanodiamonds [3, 5–9], etc. have been used as catalyst carriers; they have been shown to significantly improve catalysts activity, selectivity, and stability [1]. The nature and size of active centers as well as theirs accessibility to the substrate molecules is to a great extent determined by the carrier nature [3, 4].

The nanodiamond-based catalysts are of special interest. The nanodiamonds possess the crystalline lattice of diamond with many defects and highly polar organic groups present at the surface. Generally, the size of nanodiamond particles is of 1–10 nm depending on the preparation conditions and the purification method [10–12]. Nanodiamonds of such size are extremely stable carbon compounds. At the same time, they reveal unique sorption ability and high activity caused by the presence of functional groups at the surface: oxygen-containing hydroxyl, carbonyl, carboxyl, and ester groups; nitrogen-containing amino and amide groups; and less common methyl and methylene ones. Chemical state of these groups determines the properties of diamond particles. The small size and extremely high surface activity of nanodiamonds make then an excellent carrier for platinum group metals. On the contrary to other nanocarbon materials, nanodiamonds can be used without the oxidative pre-treatment. With detonation nanodiamonds used as carriers of the platinum group metals, platinum and palladium clusters can be obtained, 0.4–1.2 nm thick and 5 nm in diameter. It is the presence of non-compensated bonds at carbon atoms of nanodiamonds [10–13] that provides the uniformity of active centers and the largest catalytically active surface, essential for adsorption of substrates and desorption of reaction products. The nanodiamond-based catalysts have been tested in the conversion of CO to CO_2 [6, 10–12] and hydrodehalogenation of trichlorobenzenes [5, 6]. They are also promising catalysts for the decomposition of alcohols (ethanol and methanol) [13]. Noteworthily, detonation nanodiamonds are commercially available in Russia.

We have shown recently [3] that Pt- and Pd-containing nanodiamonds are more active in the catalytic liquid phase hydrogenation of nitrobenzene as compared to other platinum- and palladium-containing carbon nanomaterials such as fullerene black, carbon nanotubes and nanofibers. In this work, we report on catalytic properties of Pd/ND and Pt/ND systems in hydrogenation of nitro compounds, azomethines, unsaturated hydrocarbons and alcohols (hereafter, ND states for nanodiamond).

We prepared the Pt/ND samples containing 5, 10, 15, 20, and 25 wt % of Pt and Pd/ND samples with 3, 6, 9, 12, and 15 wt % of Pd. The total specific surface (S_{sp}) of those samples was of 263–311 $m^2 g^{-1}$, the metal surface was of 50–324 $m^2 g^{-1}$, and the size of the metal particles was of 4–5 nm.

Scheme 1.

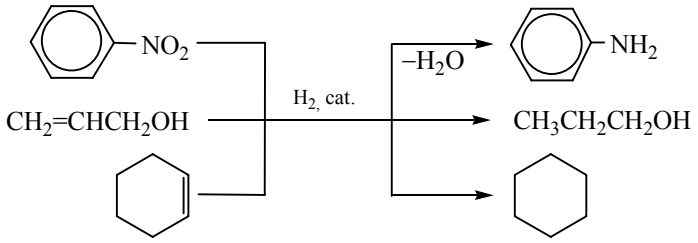

Scheme 2.

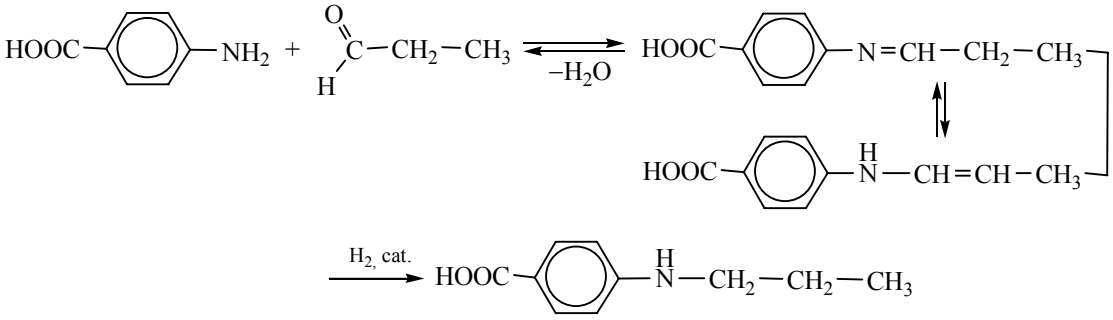

Catalytic activity of the prepared samples was tested towards hydrogenation of nitrobenzene, allyl alcohol, cyclohexene (Scheme 1), and azomethine (Scheme 2). The substrates were chosen according to their practical importance as well as to the variety of the reduced groups (NO_2, C=C, >C=N) in the chemical nature and the location in substrate.

GLC analysis of the reaction products showed that conversion of substrates was of 100%, and no by-products were found.

In hydrogenation of 4-(propylideneamino)benzoic acid, activity of the catalysts decreased with the increase in platinum or palladium content (Table 1). The samples with 5 wt % of Pt/ND (*TON* of 16.3 min^{-1}) and 3 wt % of Pd/ND (*TON* of 14.0 min^{-1}) were the most active. The samples with platinum content of 20 and 25 wt % and palladium content of 6 and 10 wt % showed close *TON* values.

In hydrogenation of nitrobenzene, hydrogen consumption was accelerated with increasing metal content in the catalyst, by 2, 3, 4, and 5 times (Fig. 1) as compared with that in the case of 3% Pd/ND indicating the increase of the active surface; however, the increase was not proportional to the amount of palladium. Thus, some part of metal was not involved in the catalytic process.

Comparison of turnover number in the case of nitrobenzene hydrogenation (Table 2) showed that the activity of catalyst decreased with increasing content of both platinum and palladium. Therefore, using the catalysts with high metal loading was not efficient.

The data on nitrobenzene hydrogenation (with 9 wt % Pd/ND and 15 wt % Pt/ND as representative examples) (Table 3) showed that the reaction rate and turnover number increased with longer catalyst activation. It could be explained by formation of more of Pd^0 that was seemingly activating the reacting hydrogen.

That hypothesis was confirmed by X-ray photoelectron spectroscopy studies of Pd/ND catalyst with 10 wt % of the metal and the specific surface area of 267 $m^2 g^{-1}$. The three samples were analyzed: the initial sample, the sample activated with hydrogen during 1 h, and the sample after hydrogenation of nitrobenzene. In the C1*s* spectrum of all three samples, the peak with bond energy of 285.18 eV was observed. It consisted of the two components, assigned to the diamond phase with sp^3 hybridization of carbon [14], and to the graphite phase with sp^2 hybridization of carbon, typical of the activated carbon (284.7 eV) [15]. In the O1s spectrum (E_b 531.14 eV), the signals of carboxyl and carbonyl forms of oxygen were found.

Moreover, the presence of oxide form corresponding to the Pd–O bond energy (529.3 eV) was confirmed.

The Pd 3*d* spectrum of the ND sample with deposited palladium is shown in Fig. 2a. The two valence states of palladium, Pd^{2+} and Pd^0, were observed in the 1.06 : 1 ratio. After reduction of the catalyst with hydrogen during 1 h (Fig. 2b), the both forms were still observed, but the Pd^{2+} : Pd^0 ratio was changed in favor of Pd^0 (to 1 : 1.23). After performing the hydrogenation reaction, only Pd^0 was observed in the spectrum (Fig. 2c). The catalyst remained active after the reaction; it could be used repeatedly without any noticeable loss of activity (Figs. 3 and 4).

In particular, Fig. 3 shows the reaction rates of hydrogenation of nitrobenzene, allyl alcohol, and cyclohexene in the presence of 10 wt % Pd/ND catalyst. Hydrogenation of the second portion of the substrates occurred faster than that of the first one; however, the subsequent portions were hydrogenated at practically the same rate. That confirmed the efficient cyclic catalytic performance of the Pd/ND sample.

The development of catalyst activity was more clearly marked when using the sample activated during 10 min (Fig. 4). In the course of hydrogenation of four portions of cyclohexene, the reaction rate was gradually increasing. In the case of nitrobenzene hydrogenation, the reaction rate was practically constant starting from the third portion of substrate. Thus, coordination of cyclohexene and nitrobenzene at the active centers of catalyst was different.

Table 1. Hydrogenation amination of propanal with 4-aminobenzoic acid in the presence of Pt/ND and Pd/ND[a]

Entry	Catalyst	S_{sp}, $m^2\ g^{-1}$	*TON*, min^{-1}
1	5 wt % Pt/ND	311	16.3
2	10 wt % Pt/ND	307	6.0
3	15 wt % Pt/ND	295	2.2
4	20 wt % Pt/ND	300	5.0
5	25 wt % Pt/ND	277	5.1
6	3 wt % Pd/ND	305	14.0
7	6 wt % Pd/ND	284	7.0
8	10 wt % Pd/ND	267	6.8
9	15 wt % Pd/ND	263	4.4

[a] *T* = 318 K, hydrogen pressure = 0.1 MPa, 30 mg of catalyst, 10 mg of $NaBH_4$, 25 mL of ethanol, 2 mmol of propanal, 2 mmol of 4-aminobenzoic acid. Error of *TON* evaluation is below 5%.

Table 2. Pd/ND and Pt/ND catalysts in hydrogenation of nitrobenzene[a]

Parameter	Pd content, wt %					Pt content, wt %				
	3	6	9	12	15	5	10	15	20	25
S_{sp}, $m^2\ g^{-1}$	305	299	293	291	263	311	307	295	288	277
S_m, $m^2\ g^{-1}$	140±70	160±40	165±40	120±40	50±20	324±60	304±40	244±40	240±40	220±40
TON, min^{-1}	127.3	89.5	82.8	73.6	65.0	29.2	12.3	42.2	32.2	25.7

[a] *T* = 318 K, hydrogen pressure = 0.1 MPa, 30 mg of the catalyst, 10 mg of $NaBH_4$, 10 mL of ethanol, 1 mmol of nitrobenzene. Error of *TON* evaluation is below 5%.

Table 3. Pd/ND catalyst in hydrogenation of nitrobenzene: effect of the activation time[a]

Catalyst	Parameters	Activation time			
		10 min	30 min	60 min	90 min
9 wt % Pd/ND	$w_{H2}\times10^4$, mol $L^{-1}\ s^{-1}$	6.3	6.8	7.0	7.5
	k, L $mol^{-1}\ s^{-1}$	481.9	569.3	547.7	576.9
	TON, min^{-1}	106.9	119.4	121.5	128.1
15 wt % Pd/ND	$w_{H2}\times10^4$, mol $L^{-1}\ s^{-1}$	8.0	7.2	8.4	8.7
	k, L $mol^{-1}\ s^{-1}$	379.5	359.0	417.4	429.3
	TON, min^{-1}	84.2	75.4	87.3	89.7

[a] *T* = 318 K, hydrogen pressure = 0.1 MPa, 30 mg of the catalyst, 10 mg of $NaBH_4$, 10 mL of ethanol, 1 mmol of nitrobenzene. Error of *TON* evaluation is below 5%.

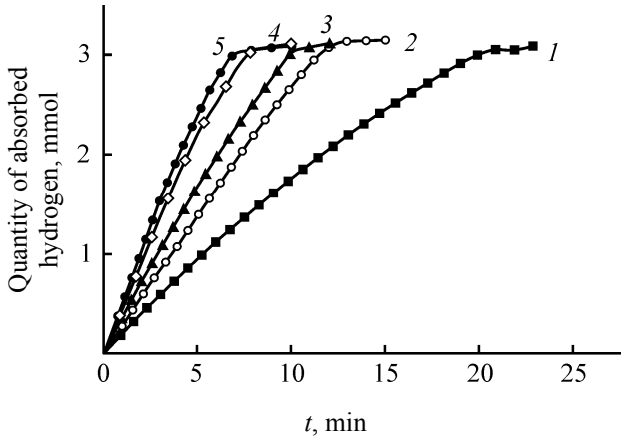

Fig. 1. Kinetics of hydrogen consumption in the course of catalytic hydrogenation of nitrobenzene in the presence of catalysts: (*1*) 3% Pd/ND, (*2*) 6% Pd/ND, (*3*) 9% Pd/ND, (*4*) 12% Pd/ND, and (*5*) 15% Pd/ND. Reaction conditions: T = 318 K, hydrogen pressure 0.1 MPa, 30 mg of the catalyst, 10 mg of $NaBH_4$, 10 mL of ethanol, 1 mmol of nitrobenzene.

The active centers of Pd/ND catalyst were most likely the clusters of Pd^0 directly participating in all the stages of hydrogenation (activation of hydrogen, adsorption of substrates, reduction of unsaturated bond or functional group, and desorption of the product). As was shown in [16], activation of hydrogen with palladium proceeded via cleavage of the covalent bond in the molecule of hydrogen to yield the chemosorbed hydrogen atoms carrying partial positive charge. It was shown as well that the rate of hydrogenation of nitrocompounds [17] and azomethines [18–20] in the presence of various palladium-containing catalysts increased with the increasing negative charge at the nitro group or at the >C=N-bond, respectively.

The total effective charges (Σq) at the reactive sites of substrates (oxygen atoms of NO_2 group, carbon atoms of >C=C< and >C=N-groups) as derived from the quantum-chemical modeling (HF/6-31G) are listed in Table 4. As the reactions were performed in ethanol, the model considered the solvent effect by taking advantage of the Polarizable Continuum Model (PCM) method. Indeed, from the results it followed that hydrogenation of the substrates was accelerated with increasing electronic density at the reaction center (–NO_2, >C=C>, or >C=N–) of the substrate (Table 4). Hydrogenation of nitrobenzene proceeded the most easily. The reaction rate constant was of 1.4, 1.8, and 13 times higher as compared to those of allyl alcohol, cyclohexene, and 4-(propylideneamino)benzoic acid hydrogenation, respectively. The trend was due to the highest steric accessibility and electronegativity of the nitro group. The allyl alcohol terminal double bond was more accessible than the double bond of cyclohexene, and the lowest reaction rate was observed in the case of the shielded azomethine group of 4-(propylideneamino)benzoic acid.

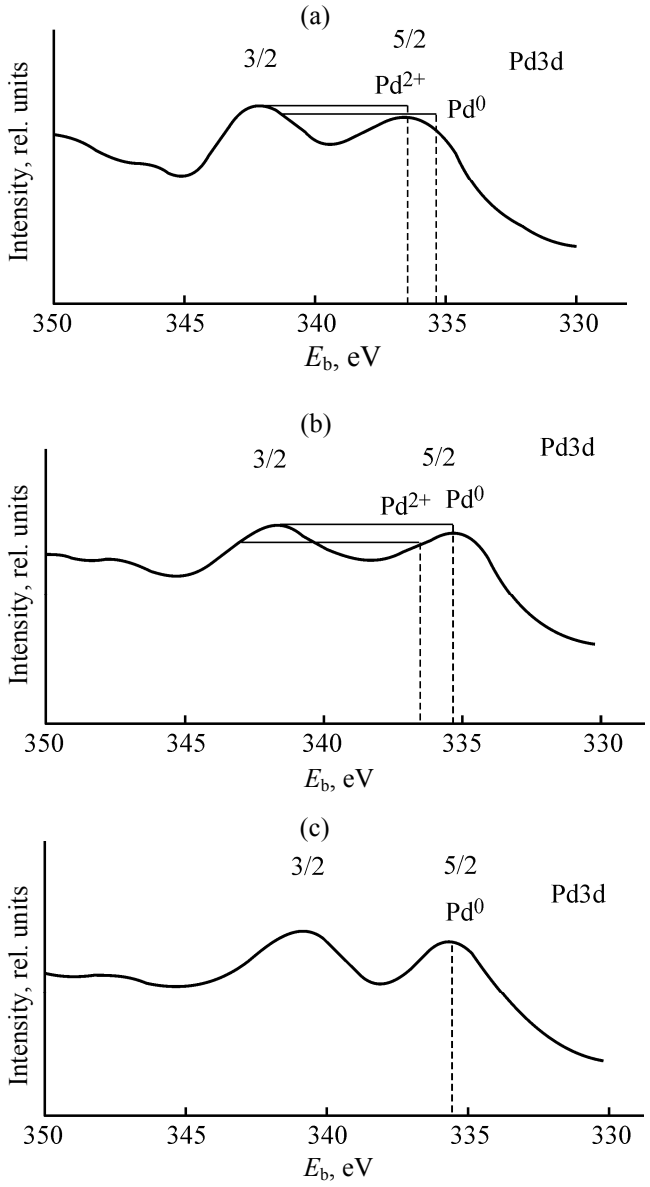

Fig. 2. Pd 3*d* XPS of the catalyst with 10 wt % of Pd/ND: (a) after treating of nanodiamonds with K_2PdCl_4; (b) after activation of catalyst with hydrogen during 1 h; (c) after hydrogenation of nitrobenzene.

Furthermore, the different mechanisms of hydrogenation of the nitro group as compared with that of >C=C, and >C=N– bonds could account for the changes in the reactivity.

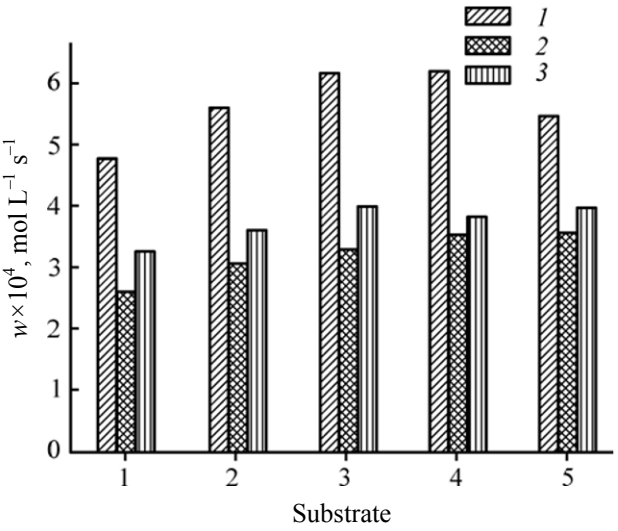

Fig. 3. Stability of 10 wt % Pd/ND catalyst in hydrogenation of nitrobenzene (*1*), allyl alcohol (*2*), and cyclohexene (*3*). Activation time 60 min. Reaction conditions: T = 318 K, hydrogen pressure 0.1 MPa, 30 mg of the catalyst, 10 mg of $NaBH_4$, 10 mL of ethanol, 1 mmol of the substrate (nitrobenzene, allyl alcohol, or cyclohexene).

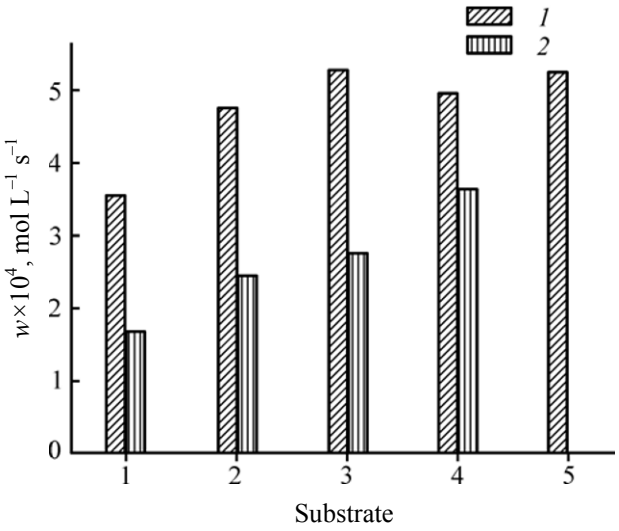

Fig. 4. Stability of 10 wt % Pd/ND catalyst in hydrogenation of nitrobenzene (*1*) and cyclohexene (*2*). Activation time 10 min. Reaction conditions: T = 318 K, hydrogen pressure 0.1 MPa, 30 mg of the catalyst, 10 mg of $NaBH_4$, 10 mL of ethanol, 1 mmol of the substrate (nitrobenzene or cyclohexene).

To conclude, the Pt/ND and Pd/ND catalysts are applicable for hydrogenation of various organic compounds (nitrocompounds, azomethines, and unsaturated hydrocarbons and alcohols). The lower metal content, of 3% Pd/ND, was found the most efficient for liquid phase hydrogenation. The studied catalysts were sufficiently stable and could be used repeatedly. Due to the commercial availability in Russia, nanodiamonds are promising for development of industrial catalysts for liquid phase hydrogenation.

EXPERIMENTAL

Nanodiamonds containing Pt and Pd were obtained as described in [11]. Detonation nanodiamonds with the specific surface area of 307–314 m^2 g^{-1} (average size of the crystalline diamond nucleus was about 4 nm) and total amount of the non-carbon admixtures below 0.5 wt % were used. Prior to application of platinum metals, 0.5–0.6 g of nanodiamonds were suspended in 70 mL of water and treated with ultrasound for 30–40 min at 40–50°C. The ultrasound intensity was of 0.5 of the maximum power of the HD 3200 ultrasonic homogenizer.

Platinum-containing nanodiamonds were prepared by reduction of aqueous solution of $H_2PtCl_4\cdot6H_2O$ with lithium formate. Aqueous suspension of nanodiamonds was heated to 40–50°C, and a mixture of $H_2PtCl_4\cdot6H_2O$ solution (without neutralization, the amount corresponded to platinum content of 5, 10, 15, 20, or 25% of the nanodiamonds mass) and lithium formate

Table 4. Activity of 10 wt % Pd/ND in hydrogenation of different organic compounds[a]

Parameter	Substrate			
	nitrobenzene	allyl alcohol	cyclohexene	4-(propylideneamino)benzoic acid
Σq, arb.units (according to Levdin)[b]	–0.703	–0.393	–0.298	–0.194
$w\times10^4$, mol L^{-1} s^{-1}	5.8	3.8	3.4	0.2
k, L mol^{-1} s^{-1}	405.9	269.6	227.2	30.9
TON[c], min^{-1}	89.6	59.9	50.4	6.8

[a] T = 318 K, hydrogen pressure = 0.1 MPa, 30 mg of the catalyst, 10 mg of $NaBH_4$, 10 mL of ethanol, 1 mmol of substrate (nitrobenzene, allyl alcohol, cyclohexene). Hydrogenation amination conditions: T = 318 K, hydrogen pressure = 0.1 MPa, 30 mg of the catalyst, 10 mg of $NaBH_4$, 25 mL of ethanol, 2 mmol of propanal, 2 mmol of 4-aminobenzoic acid. [b] HF/6-31G method, Polarizable Continuum Model (PCM), ethanol, PC GAMESS 7.1 [21]. [c] Error in *TON* evaluation is below 5%.

in (5-fold excess with respect to $H_2PtCl_4 \cdot 6H_2O$) was added. For example, the 5% Pt/ND sample was prepared from 0.066 g of $H_2PtCl_6 \cdot 6H_2O$ and 0.034 g of lithium formate dissolved in 100 mL of water.

The synthesis was performed at 40–45°C. After 20–30 min, the black precipitate was formed. The liquid phase was decanted, and the precipitate was washed with distilled water and dried at 40–60°C.

The palladium-containing nanodiamonds were prepared similarly, using K_2PdCl_4 as palladium source.

Then, the Pt/ND and Pd/ND samples were mixed with carbon in the 180:820 (mg/mg) proportion to form the homogeneous mass. That stage was introduced to minimize the subsequent weighing error.

Total specific surface of the samples was evaluated by applying the BET method to the isotherms of low-temperature nitrogen adsorption (Quantachrome Nova 3200 analyzer). The metal content in Pt/ND and Pd/ND samples was measured by X-ray microanalysis. The relative error of platinum and palladium determination was below 10%. X-ray spectral local microanalysis was performed with VEGA TS 5130MM (CamScan MV2300) TP1PT digital scanning electron microscope equipped with the secondary and backscattered electrons detector (YAG crystals) and with the energy-dispersive X-ray microanalyzer [Si(Li) semiconductor INCA Energy2 detector]. Results of the X-ray spectral microanalysis were recorded with the INCA Energy 200 software and then processed with the TP3PT software package (Institute of Experimental mineralogy of Russian Academy of Sciences). The measurements were performed at the accelerating voltage of 20 kV. The current of electrons absorbed by the reference cobalt sample was of 516–565 pA, and that in the studied samples was of 540–620 pA. The size of electronic probe at the samples surface was of 157–200 nm. The content of titanium admixture was below 0.3 wt %, and that of chlorine was below 0.1 wt %. The ash content in parent nanodiamonds was below 0.5 wt %.

Specific surface of palladium and platinum was calculated according to the equation

$$S_m = [S_{sp} - S_{ND}m_{ND}(1 - k_1k_2)]/m_m$$

with m_{ND}, content of nanodiamonds in the catalyst (g per 1 g of the catalyst); m_m, content of Pd or Pt in the catalyst; S_{ND}, specific surface of nanodiamond extrapolated to zero content of Pd or Pt; S_{sp}, total specific surface of the catalyst (nanodiamond + metal); k_1 accounted for the loss of nanodiamond surface at the contact of catalytic site and nanodiamond; k_2 accounted for the location of some part of Pd or Pt particles outside the surface of nanodiamonds (in the form of separate clusters). In [22, 23] it was shown that about 20–30% of the total metal amount formed separate clusters; therefore, k_2 was of 0.7–0.8. k_1 could be derived from $k_1 = (m_m/m_{ND})(\rho_{ND}/\rho m)$ with the average thickness of metal cluster of 0.8–1.1 nm; ρ_{ND}, specific gravity of nanodiamond, and ρ_M, specific gravity of the metal. We used the following numerical values in the calculations: $\rho_{ND} = 3.5$ g cm^{-3}, $\rho_{Pd} = 12.02$ g cm^{-3}, $\rho_{Pt} = 21.45$ g cm^{-3}, $S_{ND} = 312$ m^2 g^{-1} in the case of Pd/ND, and $S_{ND} = 313$ m^2 g^{-1} in the case of Pt/ND.

The XPS analysis of the catalysts was performed with LAS-3000 (“Riber”) device equipped with the OPX-150 hemispherical analyzer with the retentive potential. For excitation of photoelectrons, the X-ray radiation of aluminum anode AlK_α (E = 1486.6 eV) at the tube voltage of 12 kV and the emission current of 20 mA was used. The operating chamber pressure was of 5×10^{-9} Torr. The photoelectron peaks were calibrated using the C1s line of carbon with bond energy of 285 eV as the internal reference. The error of bond energy evaluation was of ±0.1 eV.

Hydrogenation of nitrobenzene, allyl alcohol, and cyclohexene (Scheme 1) was carried out as follows. The reactor was loaded with 10 mL of ethanol; then, 30 mg of catalyst and 10 mg of sodium borohydride were put under the layer of solvent, and the catalyst activation was performed during 10–120 min. After the activation, 1 mmol of the substrate was added under the hydrogen flow, and hydrogenation was carried out at 318 K and hydrogen pressure of 0.1 MPa. In the case of azomethine hydrogenation (hydrogenation amination of propanal with 4-aminobenzoic acid) (Scheme 2), the reactor was loaded with 30 mg of the catalyst and 10 mg of sodium borohydride under the layer of ethanol (5 mL), and the catalyst activation was performed during 1 h. After that, 2 mmol of 4-aminobenzoic acid and 2 mmol of propanal in 20 mL of ethanol were added, the reactor was bubbled with hydrogen, and hydrogenation was carried out at 318 K and hydrogen pressure of 0.1 MPa.

Reaction rate was evaluated by measuring the volume of the absorbed hydrogen. To compare the catalytic activity of the samples under study used the turnover number of the catalyst (*TON*, min^{-1}). *TON* showed how many moles of substrate were converted at 1 mol of metal per 1 min.

Preliminary studies showed that under the above-stated conditions, the both reactions revealed the zero

order kinetics with respect to the substrate and the first order kinetics with respect to both the catalyst and hydrogen. To confirm that the reactions proceeded in the kinetic regime, the Tile criterion (Φ) was used.

$$\Phi = R\sqrt{w/cD}$$

with R, the average diameter of catalyst particles, cm; w; the reaction rate, mol L^{-1} s^{-1}; c, concentration of substrate, mol/L; D, the diffusion coefficient, 10^{-5} cm^2 s^{-1}. The diffusion coefficient was evaluated at substrate conversion below 10% and at constant reaction rate. In the performed experiments, the Tile criterion was significantly lower than unity, $\Phi = (0.1–1.3)\times10^{-5}$. Therefore, the reactions definitely proceeded in the kinetic regime.

To estimate the catalysts stability, subsequent substrate portions were added after complete conversion of the previous portion of substrate without separation of catalyst and isolation of products from the reaction mixture.

Hydrogenation products were analyzed with standard 3700 chromatograph equipped with flame ionization detector, with 2000×3 mm glass column filled with lucopren G-1000 (5%) on Chromaton-AW-DMCS; at argon carrier gas flow rate of 0.90±0.02 L/h, evaporator temperature of 230°C, column temperature of 200°C, and injected specimen volume of 0.5–1 μL.

ACKNOWLEDGMENTS

Authors are grateful to N.N. Vershinin, V.A. Bakaev, and O.N. Efimov (Institute of Problems of Chemical Physics, Russian Academy of Sciences, Chernogolovka) for providing the samples of Pt/ND and Pd/ND and to Yu.V. Shchegol'kov (Central Scientific and Research Institute of Geological Survey of Nonferrous and Noble metals, Moscow) for performing the XPS analysis of catalysts.

The work was financially supported by Russian Foundation for Basic Research (project no. 12-03-97546-r_tsentr_a.)

REFERENCES

1. Klyuev, M.V., Volkova, T.G., and Magdalinova, N.A., *Organicheskie i gibridnye materially* (Organic and Hybrid Materials), Razumov V.F., and Klyuev M.V., Eds., Ivanovo: Ivanov. Gos. Univ., 2009, p. 147.
2. Magdalinova, N.A., Klyuev, M.V., and Volkova, T.G., Abstracts of Papers, *All-Russian Sci. and Pract. Conf. "Principles of Green Chemistry and Organic Synthesis,"* Yaroslavl': YuarGU, 2009, p. 21.
3. Magdalinova, N.A., Klyuev, M.V., Volkova, T.G., Vershinin, N.N., Bakaev, V.A., Efimov, O.I., and Korobov, I.I., *Russ. Chem. Bull*., 2011, no. 6, p. 1085.
4. Volkova, T.G., Magdalinova, N.A., and Klyuev, M.V., *Izv. Vyssh. Ucheb. Zaved., Ser. Khim*. *Khim. Tekhnol.,* 2011, vol. 56, no. 7, p. 98.
5. Golubina, E.V., Kachevsky, S.A., Lokteva, L.S., Lunin, V.V., Canton, P., and Tundo, P., *Mendeleev Commun*., 2009, vol. 19, no. 3, p. 133.
6. Golubina, E.V., Lokteva, E.S., Majouga, A.G., Lobanov, M.V., and Lunin, V.V., *Diamond Relat. Mater*., 2011, vol. 20, no. 7, p. 960.
7. Turova, O.V., Starodubtseva, E.V., Vinogradov, M.G., Sokolov, V.I., Abramova, N.V., Vul', A.Ya., and Aleksenskiy, A.E., *Catal. Commun*., 2011, vol. 12, no. 7, p. 577.
8. Magdalinova, N.A., Klyuev, M.V., Volkova, T.G., Vershinina, N.N., Bakaev, V.A., and Efimov, O.N., *Al'ternativnaya Energetika Ekologiya*, 2010, no. 3, p. 54.
9. Magdalinova, N.A., Klyuev, M.V., Volkova, T.G., Vershinin, N.N., Bakaev, V.A., and Efimov, O.N., *Al'ternativnaya Energetika Ekologiya*, 2010, no. 11, p. 113.
10. Vershinin, N.N., Aleinikov, N.N., Bakaev, V.A., and Efimov, O.N., *Ross. Nanotekh.,* 2008, nos. 5–6, p. 39.
11. Vershinin, N.N. and Efimov, O.N., RF Patent no. 2348090, 2009.
12. Vershinin, N.N., Efimov, O.N., Bakaev, V.A., Korobov, I.I., Gusev, A.L., Aleksenskiy, A.A., and Vul', A.Ya., Abstracts of Papers, *9 Biennial Int. Workshop "Fullerenes and Atomic Clusters,"* St. Petersburg, 2009, p. 239.
13. Efimov, O.N., Vershinin, N.N., Tatsiy, V.F., Gusev, A.L., and Gol'dshleger, N.F., *Al'ternativnaya Energetika Ekologiya*, 2007, no. 6, p. 98.
14. Morar, J.F., Himpsel, F.V., Hollinger, G., Jordan, J.L., Huges, G., and McFeely, F.R., *Phys. Rev*., 1986, vol. 33, p. 1340.
15. Lascovish, J.C., Giorgi, R., and Scaglione, S., *Appl. Surf. Sci*., 1991, vol. 47, p. 17.
16. Volkova, T.G. and Klyuev, M.V., *Petrol. Chem*., 1998, vol. 38, no. 3, p. 178.
17. Volkova, T.G., and Klyuev, M.V., *Neftekhimiya*, 1997, vol. 38, no. 4, p. 321.
18. Zhivotyagina, S.N., *Candidate Sci. (Chem.) Dissertation*, Ivanovo, 2005.
19. Usanova, N.N., *Candidate Sci. (Chem.) Dissertation*, Ivanovo, 2008.
20. Magdalinova, N.A., *Candidate Sci. (Chem.) Dissertation*, Ivanovo, 2009.
21. Granovsky, A.A., *PCGAMESS version 7.1.http://classic.chem.msu.su/gran/games/index.html.*
22. Vershinin, N.N., Bakaev, V.A., Efimov, O.N., Korobov, I.I., Gusev, A.L., Aleksenskii, A.E., Baidakova, M.V., and Vul', A.Ya., *Al'ternativnaya Energetika Ekologiya*, 2009, no. 9, p. 123.
23. Vershinin, N.N., Bakaev, V.A., Gusev, A.L., and Efimov, O.N., *Al'ternativnaya Energetika Ekologiya*, 2009, no. 10, p. 85.